JACS
JOURNAL OF THE AMERICAN CHEMICAL SOCIETY

Communication

pubs.acs.org/JACS

Visible-Light-Induced Hydrogen and Oxygen Formation over Pt/Au/WO_3 Photocatalyst Utilizing Two Types of Photoabsorption Due to Surface Plasmon Resonance and Band-Gap Excitation

Atsuhiro Tanaka, Keiji Hashimoto, and Hiroshi Kominami*

Department of Applied Chemistry, Faculty of Science and Engineering, Kinki University, Kowakae, Higashiosaka, Osaka 577-8502, Japan

Supporting Information

ABSTRACT: Photocatalytic H_2 and O_2 formations under visible light irradiation (λ > 400 nm) are demonstrated using Pt−Au nanopaticles for the reduction site and WO_3 for the oxidation site in solid-state Pt/Au/WO_3.

Coupling of two kinds of photocatalysts responding to visible light has recently attracted much attention as a Z-scheme process. The Z-scheme process has various advantages: (1) effective charge separation can be achieved, (2) high reduction power and deep oxidation power can be simultaneously obtained even by using visible light having less energy, and (3) various photocatalysts can be paired.[1] However, since stable photocatalysts producing H_2 under visible light irradiation are rare, only a few combinations have been reported. In most cases, mediators connecting two kinds of photocatalysts are essential. Therefore, an efficient photocatalyst for H_2 formation under visible light irradiation and a mediator-free system are needed.

It is known that gold nanoparticles (AuNPs) supported on semiconductors such as cerium(IV) oxide and titanium(IV) oxide (TiO_2) exhibit strong photoabsorption due to surface plasmon resonance (SPR).[2−11] Recently, supported Au materials have been used as visible-light-responding photocatalysts for various chemical reactions,[2] including oxidation of organic substrates,[5] selective oxidation of an aromatic alcohol to a carbonyl compound,[6] H_2 formation from alcohols,[7] and reduction of organic compounds.[8] We consider an SPR-type photocatalyst to be a strong candidate for an H_2 formation photocatalyst in the coupling of two kinds of photocatalysts. In the case of Au/TiO_2, TiO_2 only works as an electron-transportation material under visible light irradiation because TiO_2 only responds to UV light, which leads us to the idea that tungsten(VI) oxide (WO_3) can be used as a Au-supporting material. Two absorptions due to band-gap excitation of WO_3 (<450 nm) and SPR of AuNPs (450−600 nm) hardly overlap, indicating that solar light can be effectively utilized without conflict between WO_3 and AuNPs. In a Au/WO_3 sample, an efficient charge separation can be expected by coupling of the band-gap excitation of WO_3 and the SPR of AuNPs. In this case, WO_3 and supported AuNPs would work as photocatalysts for O_2 and H_2 evolution, respectively. Since AuNPs and WO_3 are in direct juncture, no mediators are required for the electron transfer in the Au/WO_3 system. However, there is one problem in the Au/WO_3 system: if electrons of Au transform to the conduction band of WO_3 through SPR, H_2 would not be formed because the potential of the conduction band of WO_3 (ca. +0.5 V_{NHE} at pH 0) is insufficient for the proton reduction (0 V_{NHE} at pH 0). Therefore, electron transfer to WO_3 should be avoided if we expect H_2 formation in the Au/WO_3 system.

In the course of our studies on SPR-type photocatalysts,[7b] we reported formation of H_2 from various compounds in aqueous suspensions of Au/TiO_2 with co-catalysts under visible light irradiation. By using the traditional photodeposition (PD) method and subsequent colloid photodeposition (CPD)[10] method, Au/TiO_2 with co-catalysts exhibiting stronger photoabsorption at around 550 nm due to SPR and higher levels of activity for H_2 production were successfully prepared. These results indicate that introduction of a co-catalyst such as platinum is important for efficient H_2 formation because the co-catalyst works as a site for H^+ reduction.

In this study, we prepared a new type of photocatalyst, i.e., Pt/Au/WO_3, in which Pt nanoparticles were loaded on Au particles. To achieve the Pt-on-Au structure, Au particles were first loaded on WO_3 by using CPD, and then Pt particles were loaded on Au particles by using PD. The Pt/Au/WO_3 sample was used for formation of H_2 and O_2 under visible light irradiation in the presence of sacrificial reagents such as biomass under mediator-free conditions. We also investigated whether two types of photoabsorption contribute to the formation of H_2 and O_2 by using an action spectrum, and we discuss the working mechanism in formation of H_2 and O_2 over Pt/Au/WO_3.

The contents of Au and Pt were fixed at 3.0 and 0.5 wt%, respectively, and the sample is designated here as Pt(0.5)/Au(3.0)/WO_3. Figure S1 shows absorption spectra of the WO_3 and Pt(0.5)/Au(3.0)/WO_3 samples. The bare WO_3 sample exhibited absorption only at λ < 500 nm due to the band-gap excitation (2.8 eV). In the spectrum of the Pt(0.5)/Au(3.0)/WO_3 sample, strong photoabsorption was observed at around 550 nm, which was attributed to SPR of the supported AuNPs.[2−11]

A transmission electron microscope (TEM) image of Au(3.0)/WO_3 prepared by CPD using the Au colloidal solution is shown in Figure 1a. Gold particles were observed in the image, indicating that AuNPs were deposited on the WO_3 surface by CPD. The average diameter of Au particles in the

Received: October 5, 2013
Published: December 27, 2013

dx.doi.org/10.1021/ja410230u | J. Am. Chem. Soc. 2014, 136, 586−589

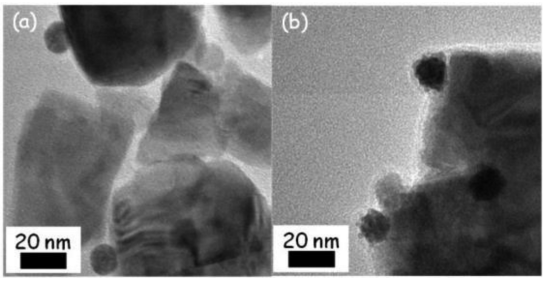

Figure 1. TEM photographs of (a) Au(3.0)/WO_3 and (b) Pt(0.5)/Au(3.0)/WO_3.

sample was determined to be 13 nm (Figure S2), which was in good agreement with the average diameter of original colloidal AuNPs before Au loading (Figure S3). In the TEM image of the Pt(0.5)/Au(3.0)/WO_3 sample (Figure 1b), small Pt particles were observed on a Au particle, indicating that deposition of Pt on Au particles can be attributed to an increase in the volume of nanoparticles.

Figure 2 shows time courses of evolution of H_2 from glycerin (10 μmol) in aqueous suspensions of Pt(0.5)/Au(3.0)/WO_3

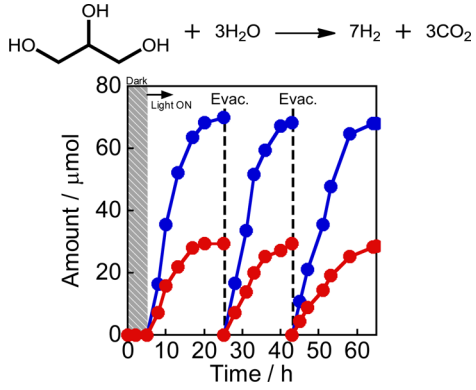

Figure 2. Time courses of evolution of H_2 (blue) and CO_2 (red) from glycerin (10 μmol) in aqueous suspensions of Pt(0.5)/Au(3.0)/WO_3 under visible light irradiation from a Xe lamp with an L-42 filter.

under visible light irradiation from a Xe lamp with an L-42 filter under a deaerated condition. Since a large amount of glycerin is formed as a byproduct in production of soap and biodiesel oil from fats and oils, effective utilization of glycerin is now keenly desired. Just after visible light irradiation, H_2 and CO_2 were evolved from suspensions of Pt(0.5)/Au(3.0)/WO_3. With increasing photoirradiation time, the amounts of H_2 and CO_2 increased linearly, and the rates of H_2 and CO_2 evolution were determined to be 6.6 and 2.8 μmol h^{-1}, respectively. Since the amount of CO_2 was in good agreement with that of H_2, glycerin was shown to have decomposed stoichiometrically to H_2 and CO_2 as shown in eq 1.

$$C_3H_5(OH)_3 + 3H_2O \rightarrow 3CO_2 + 7H_2 \quad (1)$$

No gas was evolved in the dark between 0 and 5 h, indicating that no thermocatalytic H_2 formation occurred over Pt(0.5)/Au(3.0)/WO_3 under the present conditions. To evaluate the stability of Pt/Au/WO_3 in H_2 and CO_2 production from glycerin, Pt/Au/WO_3 was used repeatedly. Visible light irradiation to the reaction mixtures after evacuation and glycerin injection (10 μmol) resulted in evolution of H_2 and CO_2 again, and the reaction proceeded with no noticeable deactivation, even for long irradiation times. The total amount of H_2 gas evolved reached ca. 210 μmol, exceeding the stoichiometric amounts of the photocatalysts (Au, 7.5 μmol, corresponding to 3.0 wt%; WO_3, 210 μmol), indicating that the H_2 production observed under the present irradiation conditions was not the result of a quantitative reagent reaction between Au and glycerin but the result of a (photo)catalytic reaction.

The combination of two kinds of light-emitting diodes (LEDs) has been shown to be useful for evaluating a composite photocatalyst consisting of two types of photocatalysts responding to light with different wavelengths.[12] To examine whether Au and WO_3 in Pt(0.5)/Au(3.0)/WO_3 contribute to H_2 formation under visible light, lights of blue and green LEDs were used solely or simultaneously as the sources (see Figure 3a).

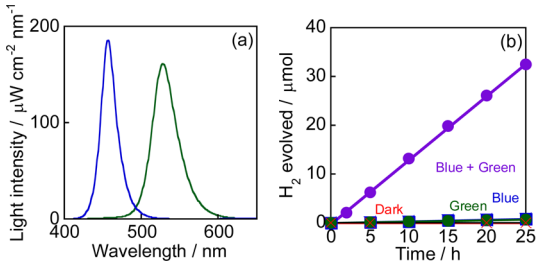

Figure 3. (a) Visible light from blue and green LEDs and (b) time course of evolution of H_2 from 2-propanol in aqueous suspensions of Pt(0.5)/Au(3.0)/WO_3 under visible light irradiation from the blue and/or green LED.

Light of the blue LED mainly induces band-gap excitation of WO_3 because the blue light hardly overlaps with SPR of AuNPs. On the other hand, light of the green LED matches photoabosorption due to SPR of Au particles but does not induce band-gap excitation of WO_3. It was preliminarily confirmed that formation of H_2 was negligible in the combination of green LED and Pt/WO_3 and the combination of blue LED and Au/WO_3 because of mismatching between the wavelength and the photoabsorption. Figure 3b shows formation of H_2 from 2-propanol in aqueous suspensions of Pt(0.5)/Au(3.0)/WO_3 under visible light irradiation from the blue and/or green LED. The amount of H_2 formed was very small under irradiation by light from either the blue or green LED. On the other hand, H_2 was formed linearly with irradiation by light from both the blue and green LEDs, and apparent quantum efficiency (AQE) was determined to be 0.40%. These results indicate that both lights were essential for H_2 formation; in other words, band-gap excitation of WO_3 and SPR of AuNPs simultaneously contribute to H_2 formation.

It is important to examine, for any given photoreaction system, the wavelength response for the reaction. In a study on an indium oxide−copper oxide (CuO) photocatalyst, we examined the action spectrum under additional irradiation by light only inducing band-gap excitation of CuO.[12] To elucidate the working mechanisms of Pt(0.5)/Au(3.0)/WO_3, the action spectrum was measured in H_2 formation from 2-propanol under additional irradiation by light from the blue or green LED. Figure 4 shows the dependence of AQE on the wavelength of incident light of monochromated visible light from a Xe lamp with light width of ±5 nm in the presence and absence of irradiation by light from the blue LED (5.9 mW

dx.doi.org/10.1021/ja410230u | J. Am. Chem. Soc. 2014, 136, 586−589

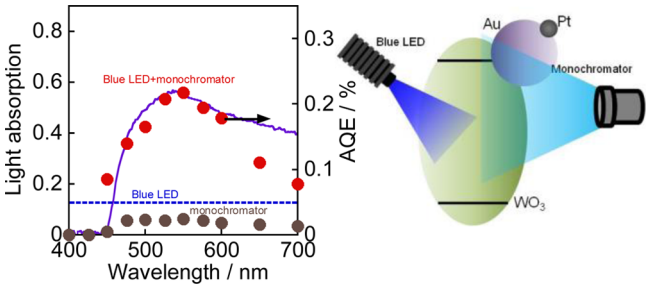

Figure 4. Dependence of rates of H_2 evolution by Pt(0.5)/Au(3.0)/WO_3 on the wavelength of incident light in the presence and absence of irradiation by light from the blue LED. The line means AQE under irradiation by light from the blue LED. The subtraction spectrum obtained from the spectra of Pt(0.5)/Au(3.0)/WO_3 and WO_3 is also shown.

cm^{-2}). The value of AQE was determined by using eq 2. The denominator of eq 2 includes all of the photons irradiated to the photocatalyst, i.e., photons from both the monochromator and blue LED.

$$\mathrm{AQE} = \frac{2 \times \text{the amount of } H_2}{\text{the amount of incident photon}} \times 100 \qquad (2)$$

The dependency was similar to the subtraction spectrum obtained from the spectra of Pt(0.5)/Au(3.0)/WO_3 and WO_3. These results indicate that H_2 formation was induced by photoabsorption due to SPR of Au. The large difference in AQE with and without the blue LED (Figure 4) indicates that light from the blue LED greatly accelerated H_2 formation. Figure 5 shows action spectra in the presence and absence of

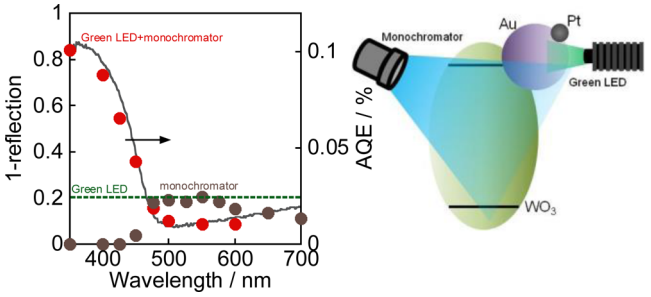

Figure 5. Dependence of rates of H_2 evolution by Pt(0.5)/Au(3.0)/WO_3 on the wavelength of incident light in the presence of irradiation by light from the blue LED. The line means AQE under irradiation by light from the green LED. The diffuse reflectance spectrum of WO_3 is also shown.

irradiation by light from the green LED (7.3 mW cm^{-2}). The dependency was similar to the absorption spectrum of WO_3, indicating that H_2 formation was also induced by photoabsorption due to the band-gap excitation of WO_3. The large gap between AQE around 400 nm in the presence and absence of the green LED shows that the band-gap excitation of WO_3 contributes to H_2 formation only when there is SPR due to AuNPs.

Since a WO_3 photocatalyst is one of the most efficient materials for O_2 formation from water under visible light irradiation, we examined water oxidation over the Pt/Au/WO_3 sample. Water oxidation activity of the Pt/Au/WO_3 sample was evaluated in the presence of hexavalent chromium (Cr^{6+} in $Cr_2O_7^{2-}$) as an electron acceptor.[11] In this O_2 evolution system, no change in the photocatalyst occurs because nothing is deposited on the photocatalyst, in contrast to the use of silver ions as electron acceptors. Rates of O_2 formation from H_2O over various photocatalysts under irradiation by both the blue and green LEDs are shown in Figure 6.

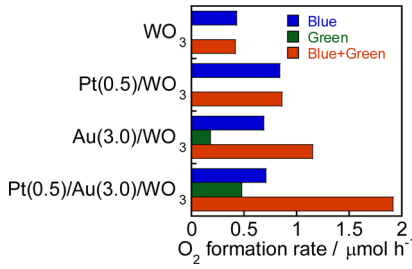

Figure 6. Rates of formation of O_2 in aqueous suspensions of various photocatalysts under visible light irradiation from the blue LED in the presence and absence of the green LED.

For comparison, results under irradiation by light from either the blue or green LED are also shown. Results for WO_3 and Pt(0.5)/WO_3 indicate that Pt worked as a co-catalyst in the reduction of Cr^{6+} [13] and that the effect of green light irradiation on O_2 formation was negligible in WO_3 and Pt(0.5)/WO_3. Since WO_3 is not photoexcited by light from a green LED, the negligible effect is reasonable. A synergistic effect of the band-gap excitation by blue light and SPR by green light was observed in O_2 formation over Au(3.0)/WO_3 and Pt(0.5)/Au(3.0)/WO_3. Results shown in Figure 6 indicate that the combination of a WO_3 semiconductor, AuNPs, and Pt co-catalyst is effective for O_2 formation and that green light, i.e., light with less energy, can be applied for acceleration of O_2 formation. In the case of Pt/Au/WO_3, AQE for water oxidation was calculated to be 0.2% under visible light irradiation from the blue and green LEDs.

It was clearly shown that both the band-gap excitation of WO_3 and the photoabsorption due to SPR of Au supported on WO_3 contributed to the photocatalytic H_2 and O_2 formation under irradiation by light from both the green and blue LEDs. The higher photocatalytic activities of Pt(0.5)/Au(3.0)/WO_3 are explained by an efficient charge separation by successful coupling of the band-gap excitation of WO_3 and the SPR of AuNPs. Based on the results shown above, the expected working mechanism for photocatalytic H_2 formation in the presence of electron donors over Pt/Au/WO_3 under visible light irradiation is shown in Scheme 1a.

Scheme 1. Expected Reaction Mechanism for Production of (a) H_2 and (b) O_2 in Aqueous Suspensions of Pt/Au/WO_3

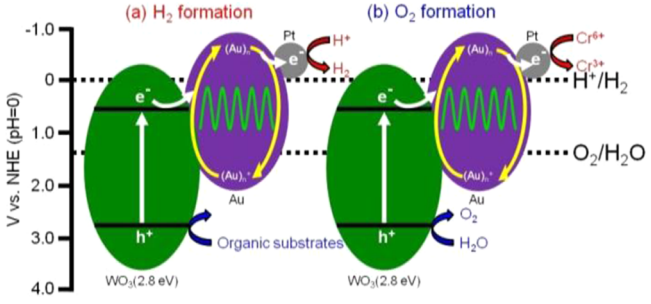

dx.doi.org/10.1021/ja410230u | J. Am. Chem. Soc. 2014, 136, 586−589

Five processes would occur: (1) the incident photons are absorbed by Au particles through their SPR excitation,[2−11] (2) electrons are transferred from the Au particles into the Pt particles, and (3) H^+ is reduced by electrons over Pt, resulting in the formation of H_2. On the other hand, (4) the incident photons are absorbed by WO_3, and holes in the valence band of WO_3 oxidize various substrates such as glycerin and 2-propanol, and (5) electrons in the conduction band of WO_3 are transferred to the electron-deficient Au particles, returning to the original state. The mechanism may be applied for the synergy effect of simultaneous irradiation by UV and visible light on H_2 formation over Au/TiO_2,[9] in which band-gap excitation of TiO_2 and SPR of Au particles are induced by UV and visible light, respectively.

Since hydrogen overvoltage of Pt metal (0.01 V[14]) is smaller than that of Au metal (0.18 V[14]), i.e., H_2 evolution over Pt is easier than that over Au, electron transfer from Au to Pt in process (2) is reasonable. If electrons are transferred to the conduction band of WO_3 in process (2), H_2 formation would not occur any more because of insufficient potential of the conduction band of WO_3 for H^+ reduction as mentioned in the second paragraph. Formation of H_2 indicates that electrons of AuNPs are transferred to Pt particles, not to the conduction band of WO_3. For comparison, another sample, Au/WO_3−Pt, in which Pt particles were loaded on WO_3 without alloying Au particles,[7b] was prepared (Figure S4) and used for H_2 formation under the same conditions (Figure S5). The Au/WO_3−Pt sample showed negligible activity, indicating that electron transfer from Au to the conduction band[4] of WO_3 (or Pt on WO_3) was predominant in this sample. Large differences in H_2 formation rate between $Pt/Au/WO_3$ and Au/WO_3−Pt (Figure S5) indicate that keeping the electron potential negative (preventing electron transfer to WO_3) in the Au/WO_3 catalyst system is important for H_2 evolution under visible light irradiation. The value of AQE over $Pt/Au/WO_3$ was, however, low, suggesting that a part of the electrons is injected to WO_3 and finally transferred to the electron-deficient Au particles.

The expected working mechanism for photocatalytic O_2 formation in the presence of an electron acceptor over $Pt/Au/WO_3$ under visible light irradiation is shown in Scheme 1b. As well as the H_2 formation system, effective charge separation accounts for the higher activity of $Pt/Au/WO_3$.

In summary, by using colloid photodeposition of Au particles on WO_3 followed by photodeposition of Pt particles onto Au particles, a $Pt/Au/WO_3$ sample was successfully prepared. The $Pt/Au/WO_3$ sample continuously yielded H_2 and CO_2 from glycerin under visible light irradiation. Results for H_2 formation under visible light irradiation from a blue and/or green LED indicate that both lights were essential for H_2 formation. The action spectrum under additional irradiation by light from the blue LED or green LED clarified that both the band-gap excitation of WO_3 and SPR of AuNPs simultaneously contribute to the H_2 formation. $Pt/Au/WO_3$ also produced O_2 by oxidation of H_2O under visible light irradiation, to which both the band-gap excitation of WO_3 and SPR of AuNPs simultaneously contributed. The SPR photocatalyst was applied for the first time to a two-step photoexcitation system through combination with WO_3. There are many variations in combination of plasmonic photocatalysts and band-gap photocatalysts. The results obtained in this study can be widely applied to design of a new type of photocatalyst utilizing both SPR and band-gap excitation.

■ ASSOCIATED CONTENT

Supporting Information

Experimental details and Figures S1−S5. This material is available free of charge via the Internet at http://pubs.acs.org.

■ AUTHOR INFORMATION

Corresponding Author

hiro@apch.kindai.ac.jp

Notes

The authors declare no competing financial interest.

■ ACKNOWLEDGMENTS

This work was partly supported by a Grant-in-Aid for Scientific Research (No. 23560935) from the Ministry of Education, Culture, Sports, Science, and Technology (MEXT) of Japan. H.K. and A.T. are grateful for financial support from Iketani Science and Technology Foundation. A.T. is grateful to the Japan Society for the Promotion of Science (JSPS) for a Research Fellowship for young scientists.

■ REFERENCES

(1) (a) Sayama, K.; Mukasa, K.; Abe, R.; Abe, Y.; Arakawa, H. *Chem. Commun.* **2001**, 2416−2417. (b) Abe, R.; Takata, T.; Sugihara, H.; Domen, K. *Chem. Commun.* **2005**, 3829−3831. (c) Abe, R.; Sayama, K.; Sugihara, H. *J. Phys. Chem. B* **2005**, *109*, 16052−16061. (d) Maeda, K.; Higashi, M.; Lu, D.; Abe, R.; Domen, K. *J. Am. Chem. Soc.* **2010**, *132*, 5858−5868. (e) Sasaki, Y.; Kato, H.; Kudo, A. *J. Am. Chem. Soc.* **2013**, *135*, 5441−5449. (f) Maeda, K. *ACS Catal.* **2013**, *3*, 1486−1503.

(2) (a) Chen, X.; Shen, S.; Guo, L.; Mao, S. S. *Chem. Rev.* **2010**, *110*, 6503−6570. (b) Navarro, R. M.; Sánchez-Sánchez, M. C.; Alvarez-Galvan, M. C.; del Valle, F.; Fierro, J. L. G. *Energy Environ. Sci.* **2009**, *2*, 35−54. (c) Zhou, X.; Liu, G.; Yu, J.; Fan, W. *J. Mater. Chem.* **2012**, *22*, 21337−21354. (d) Linic, S.; Christopher, P.; Ingram, D. B. *Nat. Mater.* **2011**, *10*, 911−921. (e) Tatsuma, T. *Bull. Chem. Soc. Jpn.* **2013**, *86*, 1−9.

(3) Tian, Y.; Tatsuma, T. *J. Am. Chem. Soc.* **2005**, *127*, 7632−7637.

(4) Furube, A.; Du, L.; Hara, K.; Katoh, R.; Tachiya, M. *J. Am. Chem. Soc.* **2007**, *129*, 14852−14853.

(5) (a) Kowalska, E.; Abe, R.; Ohtani, B. *Chem. Commun.* **2009**, 241−243. (b) Kominami, H.; Tanaka, A.; Hashimoto, K. *Chem. Commun.* **2010**, *46*, 1287−1289.

(6) (a) Naya, S.; Teranishi, M.; Isobe, T.; Tada, H. *Chem. Commun.* **2010**, *46*, 815−817. (b) Tanaka, A.; Hashimoto, K.; Kominami, H. *J. Am. Chem. Soc.* **2012**, *134*, 14526−14533.

(7) (a) Yuzawa, H.; Yoshida, T.; Yoshida, H. *Appl. Catal., B* **2012**, *115*, 294−302. (b) Tanaka, A.; Sakaguchi, S.; Hashimoto, K.; Kominami, H. *ACS Catal.* **2013**, *3*, 79−85.

(8) Ke, X.; Sarina, S.; Zhao, J.; Zhang, X.; Chang, J.; Zhu, H. *Chem. Commun.* **2012**, *48*, 3509−3511.

(9) (a) Silva, C. G.; Juarez, R.; Marino, T.; Molinari, R.; Garcia, H. *J. Am. Chem. Soc.* **2011**, *133*, 595−602. (b) Mubeen, S.; Lee, J.; Singh, N.; Kramer, S.; Stucky, G. D.; Moskovits, M. *Nat. Nanotechnol.* **2013**, *8*, 247−251. (c) Chem, J.-J.; Wu, J. C. S.; Wu, P. C.; Tsai, D. P. *J. Phys. Chem. C* **2011**, *115*, 210−216.

(10) Tanaka, A.; Ogino, A.; Iwaki, M.; Hashimoto, K.; Ohnuma, A.; Amano, F.; Ohtani, B.; Kominami, H. *Langmuir* **2012**, *28*, 13105−13111.

(11) Tanaka, A.; Nakanishi, K.; Hamada, R.; Hashimoto, K.; Kominami, H. *ACS Catal.* **2013**, *3*, 1886−1891.

(12) Sasaki, Y.; Tanaka, A.; Hashimoto, K.; Kominami, H. *Chem. Lett.* **2013**, *42*, 419−421.

(13) Xu, Y.; Chen, X. *Chem. Ind.* **1990**, *6*, 497−498.

(14) Kominami, H.; Furusho, A.; Murakami, S.-Y.; Inoue, H.; Kera, Y.; Ohtani, B. *Catal. Lett.* **2001**, *76*, 31−34.